Appl. Phys. A 92, 267–274 (2008)
DOI: 10.1007/s00339-008-4528-9

Applied Physics A
Materials Science & Processing

KOO-HYUN CHUNG*
HYUN-JOON KIM
LI-YU LIN
DAE-EUN KIM✉

Tribological characteristics of ZnO nanowires investigated by atomic force microscope

Department of Mechanical Engineering, Yonsei University, Seoul 120-749, South Korea

Received: 11 January 2008 / Accepted: 3 April 2008
Published online: 21 May 2008 • © Springer-Verlag 2008

ABSTRACT Zinc oxide (ZnO) nanowires have attracted great interest in nanodevices. In this work, the tribological characteristics of vertically grown ZnO nanowires obtained by metalorganic chemical vapor deposition were investigated by using an atomic force microscope (AFM). The ZnO nanowires were slid against flattened silicon and diamond-coated AFM probes under 50–150 nN normal force while monitoring the frictional force. The wear of the ZnO nanowires was observed by a scanning electron microscope and quantified based on Archard's wear law. Also, the wear debris accumulated on the silicon probe was analyzed by using a transmission electron microscope (TEM). The results showed that the wear of ZnO nanowires slid against the silicon probe was extremely small. However, when the ZnO nanowires were slid against the diamond-coated probe, the wear coefficients ranged from 0.006 to 0.162, which correspond to the range of severe wear at the macroscale. It was also shown that the friction coefficient decreased from 0.30 to 0.25 as the sliding cycles increased. From TEM observation, it was found that the ZnO wear debris was mainly amorphous in structure. Also, crystalline ZnO nanoparticles were observed among the wear debris.

PACS 07.79.Lh; 46.55.+d; 81.07.Bc

1 Introduction

Zinc oxide (ZnO) is an important material for applications in electronics, optoelectronic devices, and piezoelectric sensors due to its high exciton binding energy and piezoelectric and ferroelectric properties. Particularly, ZnO nanowires [1] have attracted great interest for various applications such as chemical/biomedical sensors [2, 3], UV detectors [4] and field emission displays (FEDs) [5]. Also, based on the unique ZnO nanostructures, nanocomponents such as nanobelts [6], nanorings [7], and nanosprings [8] have been introduced. Furthermore, owing to its high elastic modulus and high aspect ratio, the potential application of a ZnO nanowire as an atomic force microscope (AFM) probe has been proposed [9, 10]. As a feasibility study for this application, a topographical AFM image was successfully obtained by using a ZnO whisker glued on to the AFM cantilever [11, 12].

To understand the mechanical properties of ZnO films, an instrumented indentation technique has been widely used [13–17]. In one study, it was shown that the elastic modulus and hardness of an epitaxial ZnO thin film on *c*-axis sapphire deposited by radio frequency magnetron sputtering were 154 and 8.7 GPa, respectively [13]. However, in another study it was shown that the hardness of the ZnO epitaxial layers on *a*- and *c*-axis sapphire deposited by molecular beam epitaxy (MBE) was 5.8 and 6.6 GPa, respectively [16]. The discrepancy in the hardness values of the ZnO films could be due the nature of the deposition processes. Recently, by using an AFM-based technique, the elastic modulus of an individual ZnO nanowire was found to be 29 ± 8 GPa [17]. In addition to the mechanical properties, the tribological performance of ZnO thin films has been explored [18, 19]. The results showed that ZnO thin films have relatively low friction and long wear life. Considering the fact that wear of the AFM probe is one of the major concerns in AFM-based measurements and applications [20], the tribological characteristics of ZnO nanowires are of great importance. Recently, the wear characteristics of a vertically grown ZnO nanowire sliding against steel have been investigated. The results showed that the wear rate ranged from 0.11 to 0.29 nm/cycle [10]. However, the tribological characteristics of the ZnO nanowire at the nanoscale have not been sufficiently explored.

The motivation of this work is to better understand the tribological characteristics of a ZnO nanowire at the nanoscale. A ZnO vertical nanowire array was prepared by the metalorganic chemical vapor deposition (MOCVD) method. Sliding tests at the nanoscale were performed using an AFM under the normal force in the range of 50 to 150 nN. By comparing the geometrical shapes of the tips of the ZnO nanowires before and after the test, a quantitative wear coefficient was obtained based on Archard's wear law. Also, the frictional force was monitored during the wear experiment. Following the sliding test, the wear debris attached at the end of the AFM probe was observed by a transmission electron microscope (TEM) to understand the wear behavior of the ZnO nanowire. The experimental details and the results are described in the following sections.

✉ Fax: +82-2-312-2159, E-mail: kimde@yonsei.ac.kr
*Currently at: National Institute of Standards and Technology, Gaithersburg, MD 20899, USA

2 Experimental details

2.1 *ZnO nanowires*

Vertically aligned ZnO nanowire arrays were deposited on *c*-axis sapphire substrates in low supersaturation conditions using a MOCVD system. The low supersaturation condition was achieved by controlling the growth temperature to be as high as 870 K, which decreased the reaction rate between the zinc and oxygen. Diethylzinc with Ar carrier gas was supplied into the reactor as Zn precursor and high-purity oxygen was used as an oxidizer. The nanowire samples were supplied by the Information and Electronic Materials Research Laboratory of the Department of Materials Science and Engineering at Yonsei University. The detailed parameters for the ZnO nanowire fabrication process are described in [21]. The scanning electron microscope (SEM) images of the ZnO nanowire specimen are given in Fig. 1. Figure 1 a shows the tilted view of the specimen. It can be seen that the ZnO nanowires were well-aligned vertically. The radius of curvature at the tip of the nanowires was as small as 10 nm, which is comparable to the commercially available silicon and silicon nitride AFM probes. Thus, the sharpness of the ZnO nanowires was adequate for them to be used as AFM probes. The top view of the ZnO nanowires is shown in Fig. 1b. From this image, the radius of a nanowire was estimated to be 75 ± 18 nm. The average distance between the nanowires was approximately 170 nm.

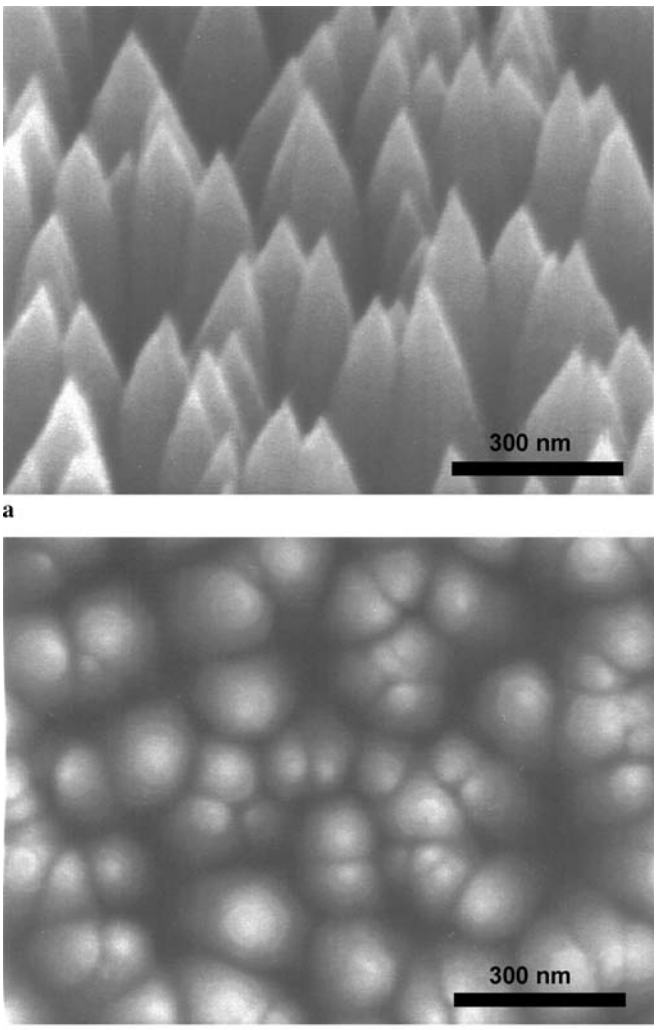

FIGURE 1 SEM images of ZnO nanowire specimen: (**a**) tilted and (**b**) top views

2.2 *Experimental method*

In order to assess the tribological characteristics of the ZnO nanowires at the nanoscale, the nanowire specimens were slid against AFM probe tips using a commercial AFM. Before the experiment, a rectangular reference mark of $40 \times 40\,\mu m^2$ was prepared on the sample and the sliding test was performed within the marked area. This allowed for convenient SEM imaging of the worn area. As for the AFM probe, silicon and diamond-coated tips were used. The nominal radius of the silicon and diamond-coated probe tips was 10 and 150 nm, respectively. However, the radius of curvature of the ZnO nanowire tip was as small as the radius of the AFM probe tip and, therefore, the AFM probe tips were flattened prior to the sliding test in order to maintain consistent contact geometry. The experimental parameters for the flattening process were determined by considering the previously reported wear coefficients of silicon and diamond-coated probes [22, 23]. As for the counter specimen used for the flattening process, hard silicon nitride deposited on silicon (100) by plasma-enhanced chemical vapor deposition (PECVD) was used.

Figure 2 shows the SEM images of the silicon and diamond-coated probes after the flattening process. From Fig. 2a, it can be seen that the silicon probe was flattened adequately. The diameter of the flattened area of the silicon probe tip was about 370 nm, which was significantly larger than the average distance between the nanowires. The inclination of the tip surface was due to the mounting angle of the cantilever holder on the AFM [22]. Furthermore, no significant wear debris was attached to the end of the silicon probe. However, the diamond-coated probe could not be flattened properly and the wear debris contamination on the probe surface was significant, as shown in Fig. 2b. This was due to the high hardness of the diamond-coated probe, which in turn generated a large amount of wear debris from the flat silicon nitride counter surface. The diameter of the diamond-coated probe was 330 nm. Also, the relatively flattened area at the tip of the probe was determined to be 140 nm, which is comparable to the average distance of the nanowires. It appeared that the flattened region of the diamond-coated probe was significantly rougher than that of the silicon probe. For comparison, the SEM image of ZnO nanowires is shown in Fig. 2b.

In order to determine the loading condition precisely, the spring constants of the AFM probes needed to be known. The normal spring constants of the silicon and diamond-coated probes were theoretically determined based on the conventional beam theory [24] after measuring the length, width, and thickness of the cantilever. The mechanical properties of silicon (100) were used for the diamond-coated probe since the diamond coating layer on the silicon cantilever substrate was significantly thinner than the cantilever thickness. The calculated normal spring constant of the silicon probe was 1.45 N/m and that of the diamond-coated probe was 2.6 N/m.

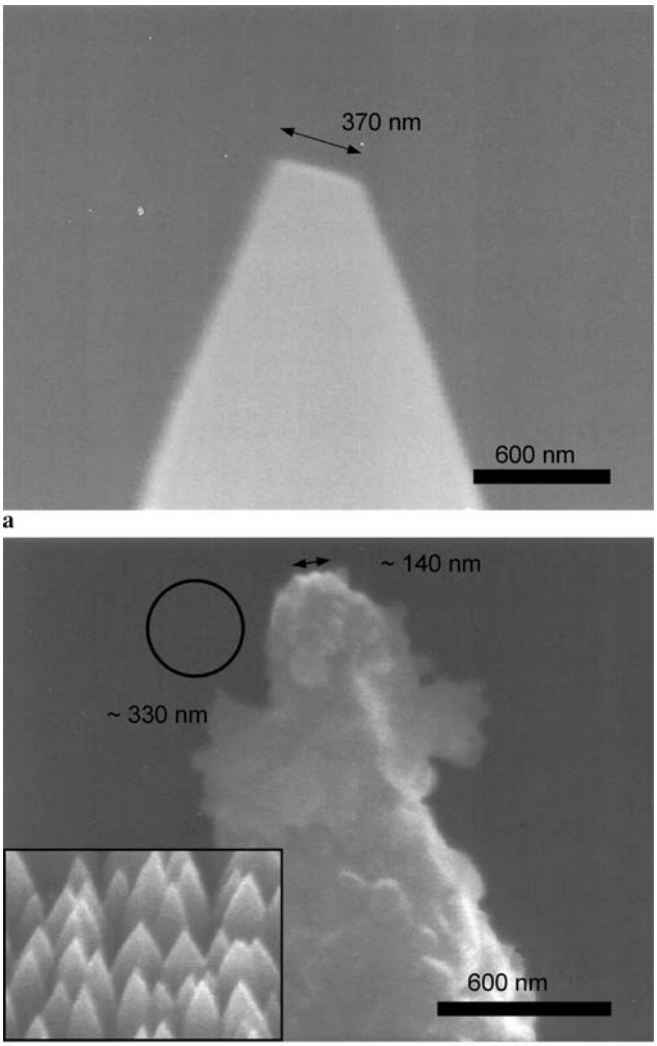

FIGURE 2 SEM images of (**a**) silicon and (**b**) diamond-coated probes used for the sliding test after the flattening process

Using these cantilevers, normal forces ranging from 50 nN to 150 nN were applied. For frictional force monitoring, the torsional spring constant of the AFM cantilevers was also calculated. The sensitivity of the AFM cantilever due to torsion was obtained by using a tip-less cantilever [25]. For the sliding test, an area of $2 \times 2\ \mu m^2$ was scanned 10 times at a sliding speed of $2\ \mu m/s$. The number of lines for each scanning was set to 256. All the experiments were conducted at room temperature and 30% relative humidity in a Class 100 clean hood.

In order to quantify the wear of the nanowire, Archard's wear law was used as given below:

$$V = k\frac{Lx}{H},$$

where V is the wear volume, L is the normal force, H is the hardness, and k is the wear coefficient. For the wear volume measurement, the geometrical changes of the ZnO nanowires were carefully observed using a SEM before and after the experiment. For the hardness of the single-crystal ZnO coated on a *c*-axis sapphire substrate a value of 8.7 GPa measured by nano-indentation was used in the calculation [13].

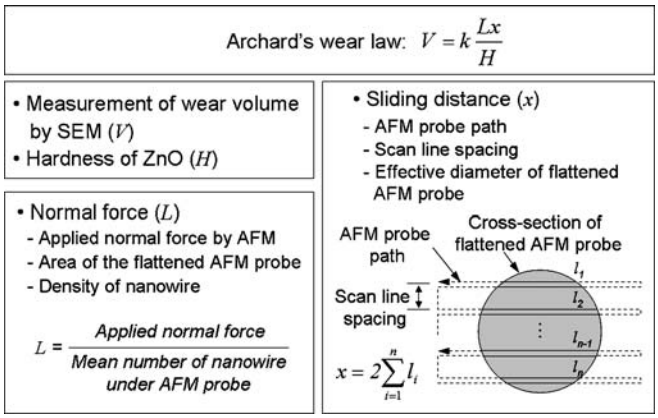

FIGURE 3 Summary of wear coefficient calculation method

For the determination of effective normal force and sliding distance, the average number of nanowires in contact with the flattened area of the AFM probe was used. Considering the spacing between the nanowires and the flattened area of the AFM probe shown in Figs. 1 and 2, the mean number of nanowires below the AFM probe was determined. For example, the average number of nanowires that were located beneath the silicon probe with a diameter of 370 nm was between 4 and 5. By assuming that the nanowires were distributed evenly with uniform heights, the average normal force on each nanowire was determined. However, the diameter of the flattened area on the diamond-coated probe was quite similar to the average distance between the nanowires. Hence, the average number of nanowires under the diamond-coated probe was set to be 1.

For the estimation of sliding distance, the number of scan lines within the flattened area of the AFM probe was obtained. Since the sliding test was performed with 256 lines over an area of $2 \times 2\ \mu m^2$, the spacing between the lines was 7.8 nm. Considering the AFM probe path, the number of scan lines within the diameter of the flattened area of the probe and the sliding distance of individual nanowires were determined. Then, the wear coefficient of the nanowires was calculated. The wear coefficient calculation procedure is summarized in Fig. 3.

After the experiment, the wear debris accumulated on the AFM probe was analyzed by using a TEM. Furthermore, chemical element analyses of the wear debris were performed by energy-dispersive X-ray analysis (EDX) inside the TEM. These analyses were performed to aid in better understanding of the tribological characteristics of the ZnO nanowires.

3 Tribological characteristics of ZnO nanowires

Sliding tests were performed by using the silicon probe prior to the diamond-coated probe. Figure 4a shows the SEM image of the ZnO nanowires after the test from the top view. The effective sliding distance of the individual ZnO nanowires was 275.6 μm. The entire region within the reference mark was carefully observed in vertical and tilted directions by a SEM. As shown in Fig. 4a, there was no significant wear of the nanowires. It was likely that the wear of the ZnO nanowires was too small to be detected by the SEM observation. Using the mechanical properties of the ZnO film

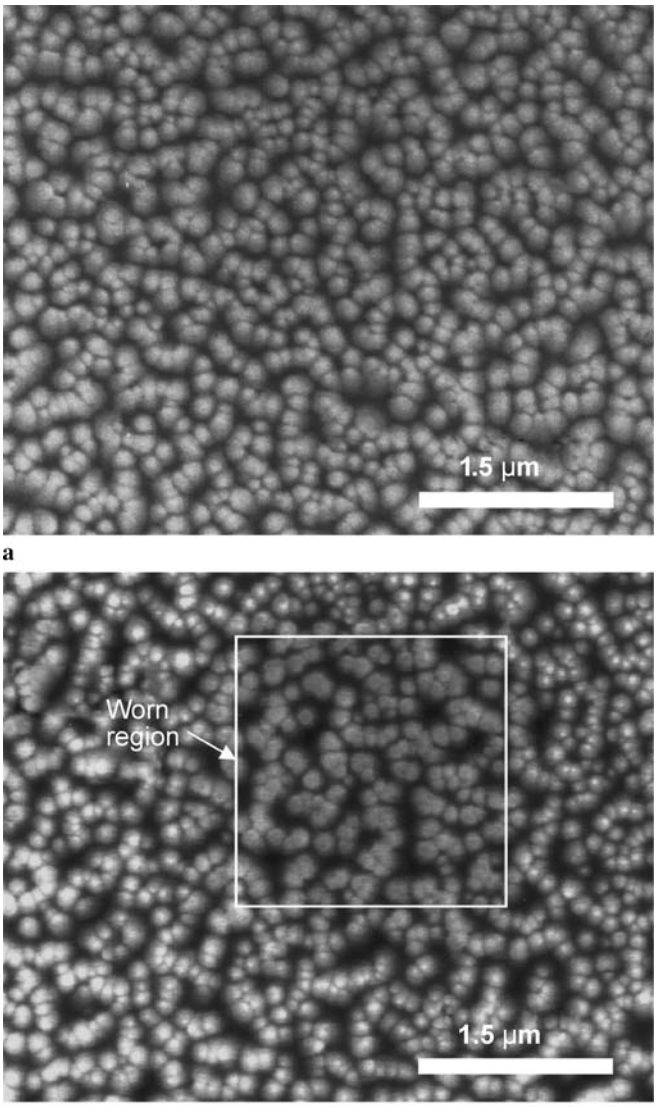

FIGURE 4 SEM images of ZnO nanowire from top view after sliding tests by using (**a**) silicon and (**b**) diamond-coated probes

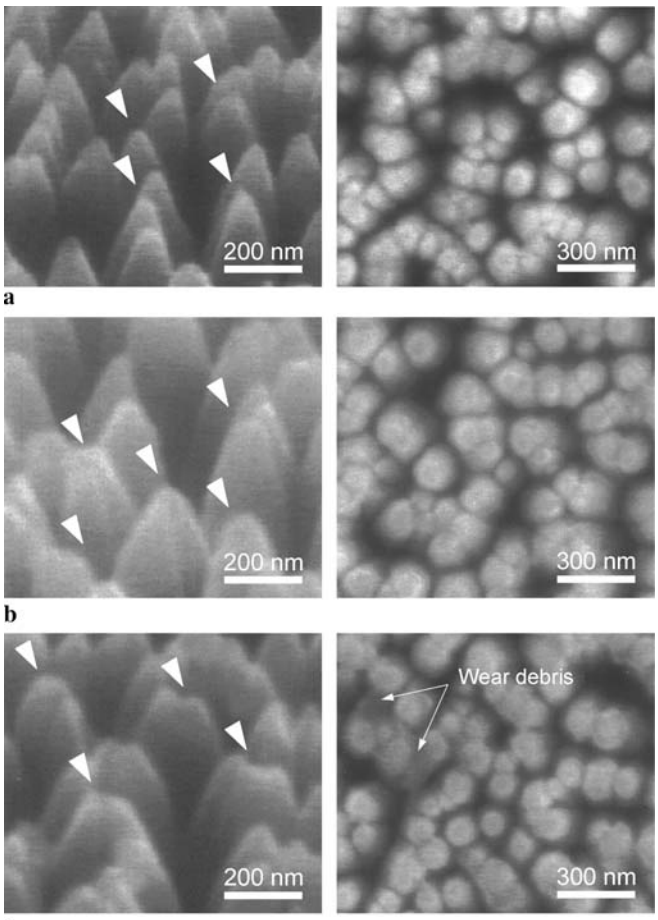

FIGURE 5 SEM images of ZnO nanowire specimen after the sliding tests under (**a**) 50 nN, (**b**) 100 nN, and (**c**) 150 nN using diamond-coated probe tip

on sapphire [13] and silicon (100), the contact pressure was estimated. The mean Hertzian contact pressure under the applied normal forces of 50, 100, and 150 nN at the initial sliding stage was calculated to be 2.9–3.1 GPa, 3.6–3.9 GPa, and 4.2–4.5 GPa, respectively. Even though the real contact pressure between the contacting asperities may be larger than the hardness of ZnO, it was likely that the pressures generated by the applied normal forces between 50 and 150 nN were not large enough to induce the detectable amount of wear by SEM. Also, the contact pressure was likely to decrease as the sliding distance increased due to wear, which in turn reduced the wear rate. Since abrasive wear is known to be one of the major wear mechanisms at micro- and nanoscale contact sliding, especially when using a sharp probe tip [26], it was expected that the difference in the hardness values of ZnO and the probe played an important role in the wear process. The hardness of the silicon ($\sim$ 10 GPa) was slightly larger than that of the ZnO film ($\sim$ 8.7 GPa). Furthermore, the hardness of the native oxide layer on the silicon probe was expected to be smaller than that of the silicon. These are probable reasons why the wear of the ZnO nanowires was too small to be observed by a SEM. In order to assess the wear of the ZnO nanowires more definitely, sliding tests using the diamond-coated probe were followed.

The wear of ZnO nanowires was clearly observed after the sliding test using the diamond-coated probe, as shown in Fig. 4b. The SEM images with high magnification are given in Fig. 5. Figure 5a–c show the SEM images of the ZnO nanowires before and after 10 cycles of sliding tests under 50, 100, and 150 nN normal force, respectively. It was evident that the ends of the nanowires became blunt and the degree of the wear increased with increase in the applied normal force. The radius of the nanowires increased from about 10 to 30–40 nm and 50–60 nm after the sliding tests under 50 and 100 nN normal force, respectively. Particularly, the nanowires were significantly flattened and the wear debris was trapped between the nanowires for the sliding test under 150 nN normal force.

By comparing the features of the ZnO nanowires before and after the test, the wear volumes were calculated. Ten nanowires were selected for the wear volume calculation. The decrease in the ZnO nanowire height under 50, 100, and 150 nN normal force was 22 ± 5.4 nm, 33 ± 6.0 nm, and 49 ± 4 nm, respectively. The wear volume under 50, 100, and 150 nN normal force was determined to be $3500 \pm 2400\,\text{nm}^3$,

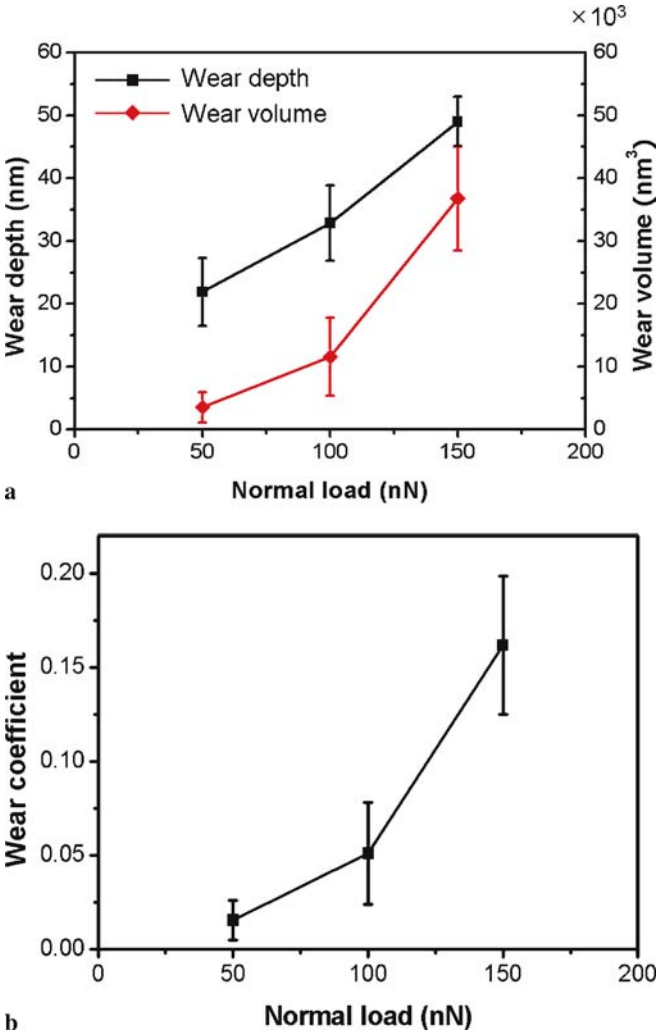

FIGURE 6 (**a**) Wear volume, wear depth, and (**b**) wear coefficient of the ZnO nanowires

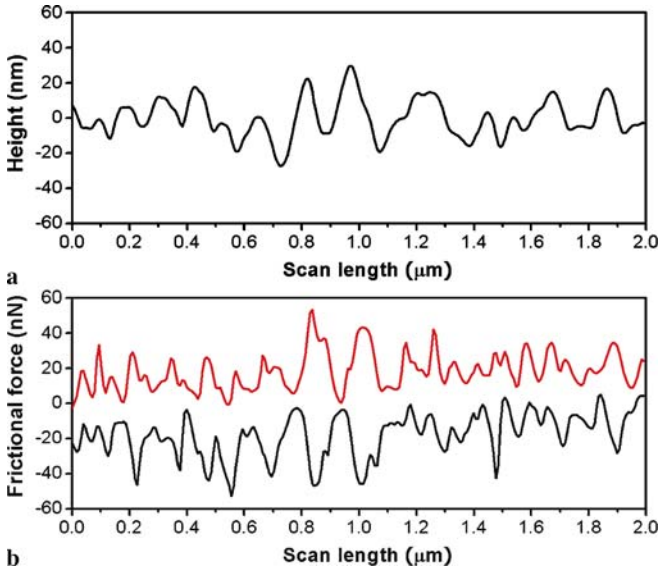

FIGURE 7 Representative (**a**) topographic and (**b**) frictional force (one cycle) profiles of the ZnO nanowire measured during the sliding test under 50 nN normal force by diamond-coated probe

$11\,600 \pm 6200\ \text{nm}^3$, and $36\,800 \pm 8400\ \text{nm}^3$, respectively. The wear depth and wear volume with respect to the applied normal force are shown in Fig. 6a. The wear depth as well as the wear volume increased as the normal force increased. For wear coefficient calculation, the sliding distance and the applied normal force for each nanowire were estimated. The sliding distance of an individual nanowire during 10 scannings within the $2 \times 2\ \mu\text{m}^2$ area with 256 lines was approximately 39.6 μm.

Using the effective normal force and sliding distance, the wear coefficient was determined to be 0.006, 0.051, and 0.162 under 50, 100, and 150 nN normal force, respectively. These wear coefficients were similar to that of the silicon AFM probe reported previously [22, 26]. Also, the orders of magnitude of the wear coefficient corresponded to severe abrasive wear at the macroscale reported in other work [27]. The wear coefficient with respect to the normal force is given in Fig. 6b. The wear coefficient increased as the normal force increased. Particularly, the wear coefficient increased by an order of magnitude as the normal force increased from 50 to 150 nN. This suggested that there was a critical pressure within this range of normal force that caused the drastic increase in the wear coefficient. The mean Hertzian contact pressure at the initial contact sliding was calculated to be 8.1, 10.2, and 11.7 GPa under 50, 100, and 150 nN applied normal force, respectively. Therefore, it was likely that significant plastic contact between the ZnO nanowires and the diamond-coated probe occurred under 100 and 150 nN normal force, which in turn induced the drastic increase in the wear coefficient. Furthermore, since the flattened area of the diamond-coated probe was quite rough, the contact pressure between the nanowires and the asperities on the diamond-coated probe may be even higher, which in turn contributed to the higher wear rate.

The frictional behavior was also monitored during the sliding experiments. Figure 7 shows representative topographic and the corresponding frictional force profiles obtained by the diamond-coated probe under 50 nN normal force. It should be noted that the topographic profile was not accurate due to the tip convolution effect. Ideally, significant peaks should not be observed in the topographic profile if only point contact occurred between the nanowires and the AFM probe. In the topographic profile shown in Fig. 7a, the number of peaks resulting from the ZnO nanowires was 13 for 2-μm scan length, which indicated that the spacing between the nanowires was about 154 nm. The average height of the 13 peaks over the 2-μm scan length was about 22 nm, which was comparable to the diameter of the tip of the ZnO nanowires. Hence, it was concluded that the contact between the ZnO nanowires and the diamond-coated probe occurred within about 22-nm distance from the tip of the nanowires.

It was expected that the frictional force would be significantly affected by mechanical interlocking between the nanowires and the AFM probe. As shown in Fig. 7b, the large variation in the frictional force corresponded quite well to the topographical profile shown in Fig. 7a. In addition, relatively small peaks that were probably due to the asperities on the flattened area of the diamond-coated probe can be seen in Fig. 7b.

Figure 8 shows the frictional force data with respect to the number of cycles under 50, 100, and 50 nN normal force.

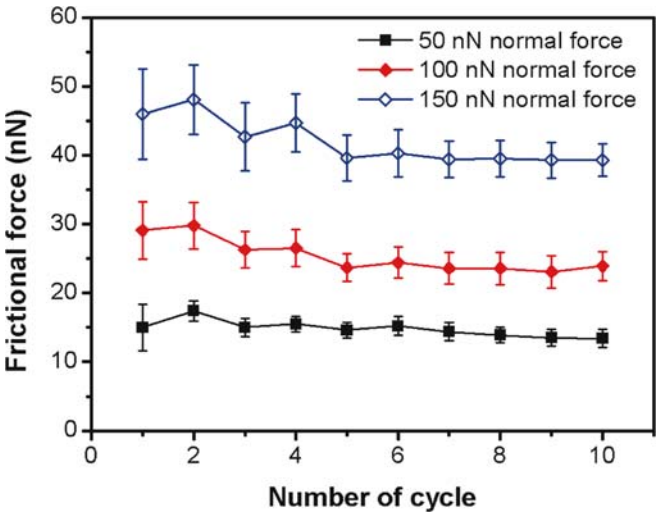

FIGURE 8 The variations of frictional force between the ZnO nanowire and the diamond-coated probe under 50, 100, and 150 nN normal force with respect to the number of cycles

The frictional force for each scan line was calculated over the forward and backward sliding motions. Then, the average values from 256 of the frictional force data were plotted with respect to the number of cycles. As expected, the frictional force increased as the applied normal force increased. Also, it was evident that the frictional force decreased slightly as the number of cycles increased. The friction coefficient decreased from about 0.30 to 0.25 as the number of cycles increased. This was probably due the decrease in the contact pressure as the wear progressed. Observation of the wear specimen using a SEM (Fig. 5c) showed that the wear debris was readily trapped between the nanowires. The wear debris trapping has the effect of reducing the plowing component of friction, thereby preventing the increase in the frictional force as sliding progresses [28]. The increase in the frictional force was relatively large when the applied force increased from 100 to 150 nN, which agrees with the wear coefficient data shown in Fig. 6.

In order to assess the AFM probe damage after the sliding tests, the probes were observed by a SEM as well as a TEM. The TEM image of the silicon probe and the SEM image of the diamond-coated probe are shown in Fig. 9. Comparing Fig. 9a with Fig. 2a, it was found that the diameter of the flattened area increased from 370 to 420 nm due to wear. Also, wear debris was accumulated around the probe. On the contrary, wear of the diamond-coated probe was not significant while contamination was severe, as shown in Fig. 9b.

The wear debris on the silicon probe was characterized by a TEM. The magnified TEM images and the diffraction patterns of 'A' and 'B' noted in Fig. 9a are shown in Fig. 10. Figure 10a shows that the structure of the wear debris in region 'A' was amorphous. The crystalline structure of ZnO was also observed in region 'B', as shown in Fig. 10b. It was likely that the ZnO particles with crystalline structure were generated due to contact sliding and eventually adhered to the AFM probe. The lattice distance of the crystalline structure was 2.48 Å, which corresponds to plane distances of {0111} and {1101}. Another crystal lattice distance measured was 2.82 Å, which corresponded to the {1010} plane distance.

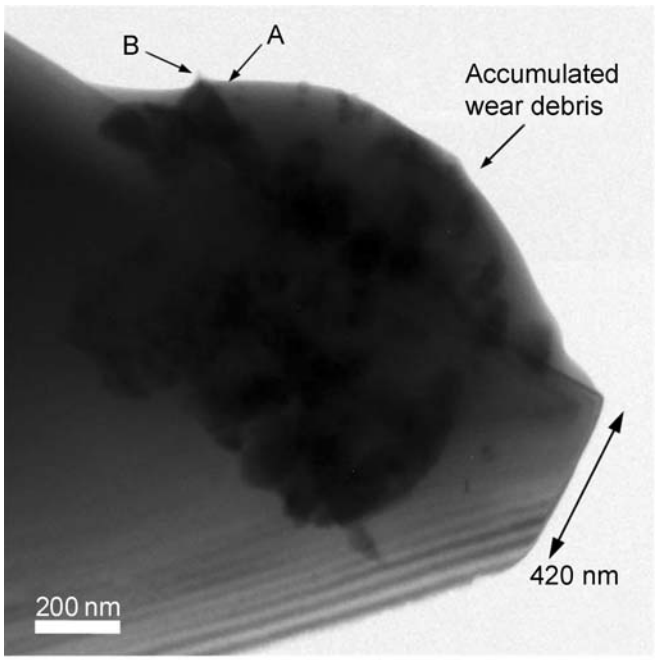

a

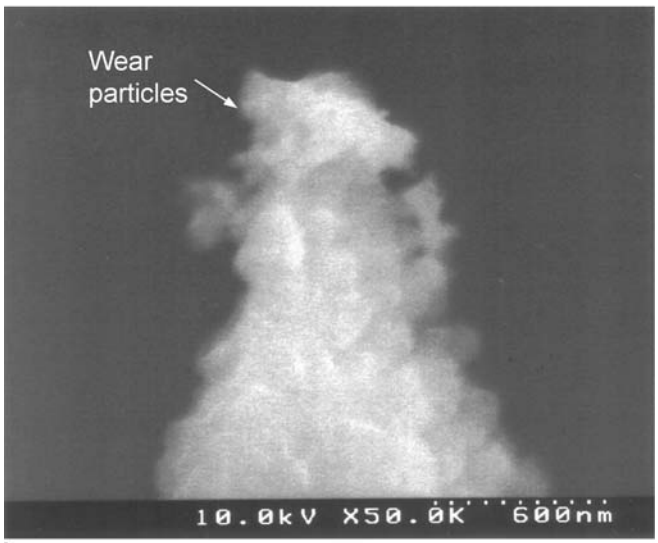

b

FIGURE 9 (**a**) TEM image of the silicon probe and (**b**) SEM image of the diamond-coated probe after the sliding test

The diffraction pattern shown in Fig. 10b agrees well with the HCP crystal structure of ZnO ([1213] zone axis). However, from careful observation of the wear debris using the TEM, it was found that the wear debris was mainly amorphous and contained a relatively small amount of crystalline structure. It was thought that both silicon and zinc were readily oxidized at the contacting interface during the sliding test, which in turn generated the amorphous wear debris. However, the presence of crystalline ZnO structure in the wear debris suggested that fracture of ZnO nanoparticles from the nanowires due to mechanical interaction may also be one of the wear mechanisms.

EDX analyses were performed following the high-resolution TEM observation to characterize the chemical composition of the wear debris. The EDX spectrum of the wear debris is shown in Fig. 11. The peaks of C, O, Si, Zn, and Cu were de-

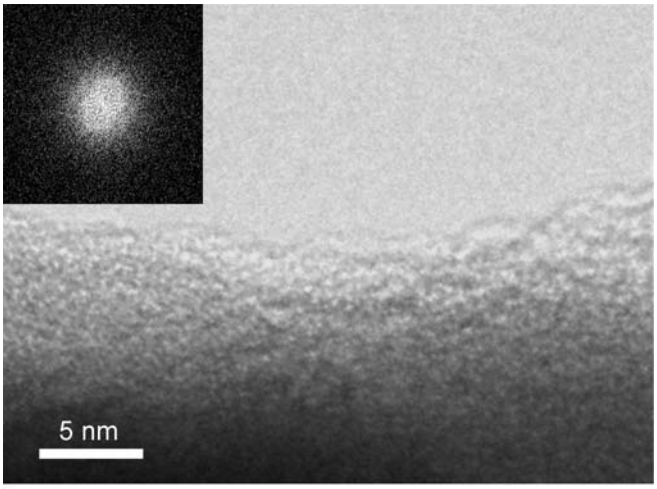

a

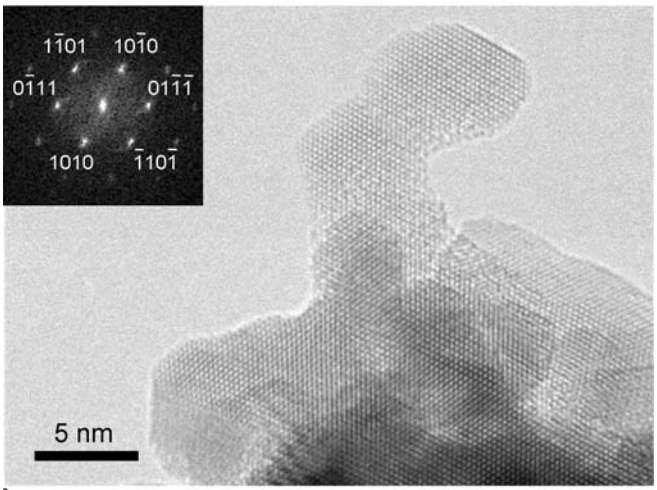

b

FIGURE 10 High-resolution TEM images and diffraction patterns of (**a**) 'A' and (**b**) 'B' in Fig. 9a

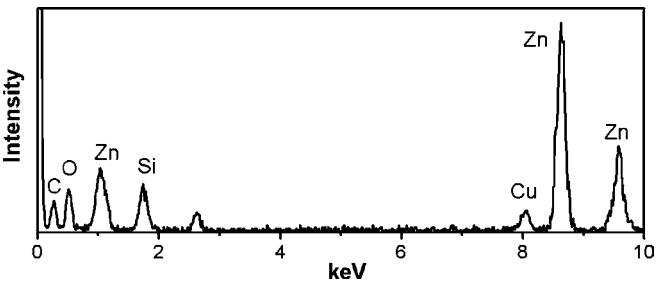

FIGURE 11 EDX spectrum of wear debris on the silicon probe

tected. Cu was from the TEM grid used in the microscopy. The EDX data suggested that the wear debris was mainly composed of the oxides of silicon as well as zinc. However, the zinc peaks were more significant than the silicon peak. Hence, it can be stated that a larger amount of ZnO was present in the wear debris than silicon.

4 Conclusions

In this work, the tribological characteristics of vertically grown ZnO nanowires were investigated by using an AFM. The sliding tests were performed by using silicon and diamond-coated AFM probe tips while monitoring the frictional force. The wear of ZnO nanowires was quantitatively assessed from SEM observations based on Archard's wear law. The wear of the ZnO nanowires slid against the silicon probe was too small to be quantified, even though a significant amount of wear debris from the ZnO was accumulated around the probe. On the other hand, the wear coefficient of ZnO nanowires slid against the diamond-coated probe was in the range of 0.006–0.162, which was similar to that of the conventional silicon probe. The high hardness and relatively high roughness of the diamond-coated probe were responsible for the severe wear of the nanowires. Although it was found that the wear coefficient increased as the applied normal force increased as expected, the relationship was not proportional. Also, it was shown that, as the wear progressed, the contact pressure decreased due to flattening of the nanowires, which in turn reduced the frictional coefficient from 0.30 to 0.25.

The wear debris accumulated on the silicon probe was analyzed using a TEM. Amorphous as well as crystalline structures of ZnO were observed in the wear debris. However, the amount of the amorphous structure was significantly larger than that of the crystalline structure. It was postulated that the amorphous wear debris was formed due to oxidation during the sliding test. Also, the fracture of crystalline ZnO nanoparticles was observed. Thus, the major wear mechanisms of the ZnO nanowires were determined to be abrasive and fracturing at the nanoscale.

ACKNOWLEDGEMENTS This work is supported by the Korea Ministry of Science & Technology through the National R&D Project for Nano Science and Technology (M1-0203-00-0031-06M0300-03110). The authors would like to thank Prof. J.M. Myung and Dr. M.-C. Jeong of the Information and Electronic Materials Research Laboratory of the Department of Materials Science and Engineering at Yonsei University for providing the ZnO nanowire specimens.

REFERENCES

1 J. Hu, T.W. Odom, C.M. Lieber, Acc. Chem. Res. **32**, 435 (1999)
2 J.X. Wang, X.W. Sun, A. Wei, Y. Lei, X.P. Cai, M. Li, Z.L. Dong, Appl. Phys. Lett. **88**, 233 106-1 (2006)
3 M.-C. Jeong, B.Y. Oh, O.H. Nam, T. Kim, J.-M. Myoung, Nanotechnology **17**, 526 (2006)
4 H. Kind, H. Yan, B. Messer, M. Law, P. Yang, Adv. Mater. **14**, 158 (2002)
5 C.J. Lee, T.J. Lee, S.C. Lyu, Y. Zhang, H. Ruh, H.J. Lee, Appl. Phys. Lett. **81**, 3648 (2002)
6 Z.W. Pan, Z.R. Dai, Z.L. Wang, Science **291**, 1947 (2001)
7 X.Y. Kong, Y. Ding, Z.L. Wang, Science **303**, 1348 (2004)
8 Z.L. Wang, J. Phys.: Condens. Matter **16**, R829 (2004)
9 W. Lee, M.-C. Jeong, J.-M. Myoung, Nanotechnology **17**, 526 (2006)
10 L.-Y. Lin, J.-M. Seo, M.-C. Jeong, K.-J. Koo, D.-E. Kim, J.-M. Myoung, Mater. Sci. Eng. A **460–461**, 370 (2007)
11 H. Kado, K. Yokoyama, T. Tohda, Rev. Sci. Instrum. **63**, 3330 (1992)
12 H. Kado, S. Yamamoto, K. Yokoyama, T. Tohda, Y. Umetani, J. Appl. Phys. **74**, 4354 (1993)
13 R. Navamathavan, K.-K. Kim, D.-K. Hwang, S.-J. Park, J.-H. Hahn, T.G. Lee, G.S. Kim, Appl. Surf. Sci. **253**, 464 (2006)
14 T.-H. Fang, W.-J. Chang, C.-M. Lin, Mater. Sci. Eng. A **452–453**, 715 (2007)
15 L.-Y. Lin, M.-C. Jeong, D.-E. Kim, J.-M. Myoung, Surf. Coat. Technol. **201**, 2547 (2006)
16 V.A. Coleman, J.E. Bradby, C. Jagadish, P. Munroe, Y.W. Heo, S.J. Pearton, D.P. Norton, M. Inoue, M. Yano, Appl. Phys. Lett. **86**, 203 105-1 (2005)
17 J. Song, X. Wang, E. Riedo, Z.L. Wang, Nano Lett. **5**, 1954 (2005)
18 J.J. Nainaparampil, J.S. Zabinski, S.V. Prasad, J. Vac. Sci. Technol. A **17**, 1787 (1999)

19 S.V. Prasad, J.S. Zabinski, Wear **203–204**, 498 (1997)
20 K.H. Chung, Y.H. Lee, D.-E. Kim, J. Yoo, S. Hong, IEEE Trans. Magn. **41**, 849 (2005)
21 M.C. Jeong, B.Y. Oh, W. Lee, J.-M. Myoung, J. Cryst. Growth **268**, 149 (2004)
22 K.-H. Chung, Y.-H. Lee, D.-E. Kim, Ultramicroscopy **102**, 161 (2005)
23 K.-H. Chung, D.-E. Kim, Ultramicroscopy **108**, 1 (2007)
24 S.P. Timoshenko, J.N. Goodier, *Theory of Elasticity* (McGraw Hill, New York, 1987)
25 G. Bogdanovic, A. Meurk, M.W. Rutland, Colloid Surf. B **19**, 397 (2000)
26 K.H. Chung, D.-E. Kim, Tribol. Lett. **15**, 135 (2003)
27 E. Rabinowicz, *Friction and Wear of Materials* (Wiley-Interscience, New York, 1995)
28 D.-E. Kim, K.H. Cha, I.H. Sung, J. Bryan, Ann. CIRP **51**, 495 (2002)